

**REPRINT with MINOR REVISIONS**

# **Calibration of the bunched exponential distribution of arrival headways**

***Reference:***

AKÇELIK, R. and CHUNG, E. (1994). Calibration of the bunched exponential distribution of arrival headways. *Road and Transport Research* 3 (1), pp 42-59.

**June 2003**

**© Akcelik & Associates Pty Ltd**

**DISCLAIMER:** The readers should apply their own judgement and skills when using the information contained in this paper. Although the author has made every effort to ensure that the information in this report is correct at the time of publication, Akcelik & Associates Pty Ltd excludes all liability for loss arising from the contents of the paper or from its use. Akcelik and Associates does not endorse products or manufacturers. Any trade or manufacturers' names appear in this paper only because they are considered essential for the purposes of this document.

---

# Calibration of the bunched exponential distribution of arrival headways

Rahmi Akçelik and Edward Chung

## ABSTRACT

The estimation of arrival headways is fundamental to the modelling of gap acceptance processes for estimating capacities of sign-controlled traffic streams, roundabout entry streams and filter turns at signalised intersections. It is also essential in modelling both vehicle-actuated signal timings and queuing at all types of intersections for performance prediction.

This paper considers a class of arrival headway distributions known as negative exponential, shifted negative exponential and bunched exponential. A description of the bunched exponential arrival headway distribution is presented, and the results of its calibration using real-life data for single-lane traffic streams and simulation data for multi-lane streams are given. Examples of gap-acceptance capacities and delays predicted by different exponential headway distributions are also presented.

Although the bunched exponential distribution is relatively new and its use less common, it has been found to be more realistic than the negative exponential and shifted negative exponential distributions. Its general use in traffic modelling is recommended.

---

**Correspondence:** Rahmi Akçelik  
Director, Akcelik & Associates Pty Ltd,  
P O Box 1075 G, Greythorn Victoria, Australia 3104  
Tel: +61 3 9857 9351, Fax: + 61 3 9857 5397  
[rahmi@akcelik.com.au](mailto:rahmi@akcelik.com.au)



### Abbreviations and notation

M1	Model 1 for estimating arrival headway distributions: <i>negative exponential</i>
M2	Model 2 for estimating arrival headway distributions: <i>shifted negative exponential</i>
M3	Model 3 for estimating arrival headway distributions: <i>bunched exponential</i>
M3A	Model M3 with Akçelik's exponential model for estimating the proportion of free (unbunched) vehicles
M3T	Model M3 with Tanner's linear model for estimating the proportion of free (unbunched) vehicles
b	Bunching factor in the exponential model for estimating the proportion of free (unbunched) vehicles
d	Average delay per vehicle (seconds)
$d_m$	Minimum gap-acceptance delay experienced by an opposed (minor / entry) movement
f(t)	Probability density function of arrival headways (probability of a headway of t seconds)
F(t)	Cumulative distribution function of arrival headways (probability of a headway less than t seconds)
h	Headway (the time between passage of the front ends of two successive vehicles at a detection point) (seconds)
$h_a$	Average arrival headway (= $1 / q$ ) (seconds)
$h_s$	Saturation headway (= $1 / s$ ) (seconds)
q	Arrival flow rate: average number of arrivals per unit time (veh/s or veh/h)
$q_t$	Total arrival flow rate in all lanes (veh/s or veh/h)
Q	Capacity (veh/s or veh/h)
s	Saturation (queue discharge) flow rate (veh/h)
t	Time (seconds)
T	Duration of the flow (design or analysis) period
x	Degree of saturation (flow/capacity ratio)
$\alpha$	Mean critical gap in a gap-acceptance process (seconds)
$\beta$	Follow-up headway of the entry stream in a gap-acceptance process (seconds)
$\Delta$	Minimum arrival (intra-bunch) headway in a single-lane or multi-lane traffic stream (seconds)
$\phi$	Proportion of free (unbunched) vehicles in a traffic stream (proportion bunched = $1 - \phi$ )

## Introduction

The estimation of arrival headways is fundamental to the modelling of all aspects of traffic. Important applications include modelling of:

- (a) gap acceptance processes for estimating capacities of sign-controlled traffic streams, roundabout entry streams and filter turns at signalised intersections (e.g. Akçelik 1981, 1990; Akçelik and Troutbeck 1991, Troutbeck 1986, 1989, 1991);
- (b) queuing at all types of intersections for predicting delays, queue lengths and stop rates (e.g. Akçelik 1981, 1990; Akçelik and Chung 1994);
- (c) extension times for estimating green times and cycle time at vehicle-actuated signals (Akçelik 1994, 1995; Lin 1982a,b); and
- (d) uninterrupted traffic flows on freeways and rural roads - see May (1990) for a brief discussion.

This paper considers the following class of *exponential* arrival headway distribution models:

Model 1 (M1): *negative exponential*,

Model 2 (M2): *shifted negative exponential*, and

Model 3 (M3): *bunched exponential*.

The simple negative and shifted negative exponential distributions are extensively discussed and used in the literature. On the other hand, the bunched exponential distribution is relatively new and, while more realistic, its use is less common. In particular, the bunched exponential distribution offers improved accuracy in the prediction of small arrival headways (up to about 12 seconds), which is important for most urban traffic analysis applications.

A description of the bunched exponential arrival headway distribution is presented, as well as results of its calibration using real-life data for single-lane traffic streams and simulation data for multi-lane streams. Examples of gap-acceptance capacities and delays predicted by different exponential headway distributions are also presented.

## Bunched exponential distribution

The bunched exponential distribution of arrival headways (M3) was proposed by Cowan (1975). It was used extensively by Troutbeck (e.g. 1986, 1989, 1991) for estimating capacity and performance of roundabouts and other unsignalised intersections. A special case of the model was previously used by Tanner (1962, 1967) for unsignalised intersection analysis. The M1 and M2 models can be derived as special cases of the M3 model through simplifying assumptions about the bunching characteristics of the arrival stream.

The M1 and M2 models are more commonly used in the traffic analysis literature as models of *random arrivals*. Alternative headway distribution models such as *Pearson Type III*, *Erlang*, *Gamma*, *lognormal* and various *composite* models (*exponential*, *hyperlang*) have been considered in the literature to overcome the shortcomings of models M1 and M2 in predicting headway probabilities for small headways and for high arrival flow rates. Useful references on arrival headway distributions for road traffic analysis include Ashton (1966), Drew (1968),

Gerlough and Huber (1975), Greenshields and Weida (1978), Haight (1963), May (1990).

The M3 model overcomes the shortcomings of the M1 and M2 models in representing real-life traffic characteristics, yet retains the simplicity of those models. In recent work, the M3 model was used successfully for deriving various formulae for the analysis of actuated signal operations (Akçelik 1994 and 1995). The model can be used consistently for all urban traffic analyses (gap acceptance modelling at signalised and unsignalised traffic facilities, modelling of traffic performance, etc.) to replace the M1 and M2 models.

The cumulative distribution function,  $F(t)$ , for the bunched exponential distribution of arrival headways, representing the probability of a headway less than  $t$  seconds in a single-lane or multi-lane traffic stream, is given by:

$$\begin{aligned} F(t) &= 1 - \varphi e^{-\lambda(t-\Delta)} && \text{for } t \geq \Delta \\ &= 0 && \text{for } t < \Delta \end{aligned} \quad (1)$$

where:

$\Delta$  = minimum arrival (intra-bunch) headway (seconds),

$\varphi$  = proportion of free (unbunched) vehicles, and

$\lambda$  = a decay parameter:

$$\lambda = \varphi q_t / (1 - \Delta q_t) \quad (1a)$$

where  $q_t$  is the total arrival flow in all lanes of the traffic stream (in veh/s).

According to the model, the traffic stream consists of:

- (a) *bunched* vehicles with all intra-bunch headways equal to the minimum arrival headway,  $\Delta$  (the proportion of bunched vehicles =  $1 - \varphi$ ); and
- (b) *free (unbunched)* vehicles with headway greater than the minimum arrival headway,  $\Delta$  (thus, the proportion of free vehicles,  $\varphi$ , represents the unbunched vehicles with randomly distributed headways).

It is emphasised that:

- (i)  $\Delta$  is a minimum *arrival* headway, and is not necessarily the same as  $h_s$ , the *saturation* headway ( $h_s = 1 / s$ , where  $s$  = saturation flow or queue discharge rate); and
- (ii) the bunched exponential model implies a geometric distribution of bunch sizes and an exponential distribution of gaps between bunches (Cowan 1975), and therefore does not represent platoons (bunches) of traffic formed at traffic signals.

The complementary function,  $1 - F(t)$ , representing the probability of a headway greater than or equal to  $t$  seconds, is given by:

$$\begin{aligned} 1 - F(t) &= \varphi e^{-\lambda(t-\Delta)} && \text{for } t \geq \Delta \\ &= 1 && \text{for } t < \Delta \end{aligned} \quad (2)$$

The probability density function of arrival headways for the bunched exponential model, representing the probability of a headway of  $t$  seconds, is:

$$\begin{aligned} f(t) &= \varphi \lambda e^{-\lambda(t-\Delta)} && \text{for } t > \Delta \\ &= 1 - \varphi && \text{for } t = \Delta \\ &= 0 && \text{for } t < \Delta \end{aligned} \quad (3)$$

### M1 and M2 models

The M1 and M2 models can be derived from the M3 model by setting the bunching parameters as follows.

Negative exponential (M1) model:

$$\Delta = 0 \quad \text{and} \quad \varphi = 1 \quad (\text{therefore } \lambda = q_t) \quad (4)$$

Shifted negative exponential (M2) model:

$$\varphi = 1 \quad (5)$$

### Discussion

Thus, models M1 and M2 assume no bunching for all levels of arrival flows. On the other hand, model M3 can be used either with a known (measured) value of  $\varphi$ , or more generally, with a value of  $\varphi$  estimated as a function of the arrival flow rate.

### M3A and M3T models

The following relationship was derived as a general formula for estimating the proportion of free vehicles in the traffic stream ( $\varphi$ ) by generalising the bunching *implied* by the negative exponential model (Akçelik 1994, 1995):

$$\varphi = e^{-b \Delta q} \quad (6)$$

where  $b$  is a bunching factor,  $\Delta$  is the minimum arrival (intra-bunch) headway, and  $q$  is the arrival flow rate (veh/s). An empirical relationship of a similar form ( $\varphi = e^{-b' q}$  where  $b' = 6$  to  $9$ ) was previously used by Brilon (1988) based on the earlier work by Jacobs (1979). The same empirical relationship has been used by Sullivan and Troutbeck (1993). Neither reference was sighted at the time of writing this paper.

The M3 model with estimates of  $\varphi$  obtained from *Equation (6)* will be referred to as the **M3A** model.

The following linear model for the proportion of free vehicles was used by Tanner (1962 and 1967):

$$\varphi = 1 - \Delta q \quad \text{for } q < 1 / \Delta \quad (7)$$

The M3 model with estimates of  $\varphi$  obtained from *Equation (7)* will be referred to as the **M3T** model.

More general form of the linear  $\phi$  -  $q$  models can be considered for calibrating real-life data. The AUSTRROADS (1993) roundabout guide uses a linear model that has been generalised in SIDRA 4.07 (Akçelik 1991; Akçelik and Besley 1992) as  $\phi = a(1 - \Delta q)$  where  $a$  is a constant (see *Equation (9)*).

## Discussion

Both M3A and M3T models assume that the proportion of free vehicles decreases, i.e. the proportion of bunched vehicles increases, with increasing arrival flow rate. They predict zero bunching ( $\phi = 1.0$ ) at very low flows. While the M3T model assumes  $\phi = 0$  at  $q = 1 / \Delta$ , the M3A model yields non-zero values of  $\phi$  at high flows. This is discussed in the following section.

For the work reported in Akçelik (1994), the M3A model was used with the parameter values of  $\Delta = 2.0$  s and  $b = 1.5$  for the single-lane case,  $\Delta = 1.0$  s and  $b = 1.0$  for the 2-lane case, and  $\Delta = 0.5$  s and  $b = 1.0$  for cases with more than two lanes. The bunching factor of  $b = 1.5$  for the single-lane case was derived as an approximation to the values predicted by the Tanner model (see *Equation (7)*). The bunching factors for multi-lane cases were derived through comparison of the lane-by-lane treatment with the treatment of arrival flows in all lanes as a *single stream*.

## Calibration

Further research was carried out for better calibration of the M3A model using real-life and simulation data. Calibration of the M3A model involved determination of a minimum arrival headway ( $\Delta$ ) and a bunching factor ( $b$ ) in *Equation (6)* that give:

- (a) a reasonable fit for the proportion of bunched vehicles (*Equation (6)*); and more importantly,
- (b) the best fit for the resulting headway distribution (*Equation (1)*).

The calibration process was carried out using real-life data for the single-lane case and simulated data for the multi-lane case. Note that the choice of  $\Delta$  affects the proportion of unbunched ( $\phi$ ) used in the process of calibration.

### Single-lane traffic surveys

The calibration of the model for single-lane traffic was based on field data collected using ARRB's VDAS vehicle detection system with treadle detectors (Leschinski and Roper 1993) at the following sites in Melbourne that represent a variety of traffic conditions. The VDAS system was used in the *individual vehicle* mode giving headway, speed and vehicle type data (a total of about 29,000 headways).

#### Site 1 (Ferntree Gully Road in Scoresby):

Uninterrupted flow conditions at a midblock location Eastbound between Jells Road and Nyadale Drive; two-lane traffic; headways in the shoulder-side lane recorded; distance to the nearest major upstream intersection (Jells Road; signalised) approximately 2.1 km; distance to the nearest major downstream intersection (Nyadale Drive; signalised) approximately 1.1 km; speed limit 80 kph; 15-min flow rates in the range 456 to 1264 veh/h; heavy vehicle percentages in the range 5 to 20 per cent; total of 14,087 headways.

**Site 2 (Fitzsimons Lane in Templestowe):**

Uninterrupted flow conditions at a midblock location Southbound between Porter Street and Main Road; two-lane traffic; headways in the shoulder-side lane recorded; distance to the nearest major upstream intersection (Main Road; roundabout) approximately 1 km; distance to the nearest major downstream intersection (Porter Street; roundabout) approximately 1.4 km; speed limit 80 kph; 15-min flow rates in the range 8 to 1208 veh/h; heavy vehicle percentages in the range 8 to 13 per cent; total of 12,235 headways.

**Site 3 (Clarinda Road in Clayton South):**

Uninterrupted flow conditions on the Southbound approach to the Clarinda Road - Bourke Road roundabout; single-lane traffic; distance to the give-way line approximately 180 m; distance to the nearest major upstream intersection (Bunney Road; roundabout) approximately 0.6 km; speed limit 60 km/h; 15-min flow rates in the range 352 to 584 veh/h; about 10 per cent heavy vehicles; total of 1052 headways.

**Site 4 (Bourke Road in Clayton South):**

Uninterrupted flow conditions on the Eastbound approach to the Clarinda Road - Bourke Road roundabout; single-lane traffic; distance to the give-way line approximately 180 m; distance to the nearest major upstream intersection (Old Dandenong Road; sign-controlled) approximately 0.4 km; speed limit 60 km/h; 15-min flow rates in the range 348 to 556 veh/h; about 9 per cent heavy vehicles; total of 1016 headways.

**Site 5 (Springvale Road in Glen Waverley):**

Headways of unqueued vehicles measured just past the stop line Southbound at the signalised intersection with Waverley Road; three lanes of through traffic; headways in the middle lane measured; distance to the nearest major upstream intersection (Kingsway; signalised) approximately 0.6 km; distance to the nearest major downstream intersection (Ferntree Gully Road; signalised) approximately 1.6 km; speed limit 70 km/h; 5-min flow rates in the range 816 to 1008 veh/h; about 8 per cent heavy vehicles; total of 274 headways.

**Site 6 (Stephensons Road in Mount Waverley):**

Headways of unqueued vehicles measured just past the stop line Northbound at the signalised intersection with Waverley Road; two lanes of through traffic; headways in the centre lane measured; distance to the nearest major upstream intersection (Ferntree Gully Road; signalised) approximately 1.6 km; distance to the nearest major downstream intersection (Virginia Street; signalised) approximately 0.7 km; speed limit 60 kph; 5-min flow rates in the range 732 to 888 veh/h; about 2 per cent heavy vehicles; total of 220 headways.

Note: Five-minute flow periods were used at Sites 5 and 6 due to the small amount of data available at these sites.

**Multi-lane traffic simulations**

Data for multi-lane cases were generated by simulating headways in individual lanes and measuring the headways of vehicles (cars only) across all lanes. In simulation, the headways in individual lanes were generated using the calibrated M3A model for single lanes (*Equation 8a*). Both equal and unequal lane utilisation cases were considered. The following conditions were simulated (total of about 367,500 headways were generated):

**Two lanes:** Equal lane flows with total flow rates of 450, 900 and 1350 veh/h per lane; unequal flow cases with total flow rates of 900 veh/h (lane flow split: 33%, 67%), 1800 (lane flow split: 25%, 75%), and 2700 (lane flow split: 39%, 61%);

**Three lanes:** Equal lane flows with total flow rates of 450, 900 and 1350 veh/h per lane; unequal flow cases with total flow rates of 1350 veh/h (lane flow split: 22%, 22%, 56%), 2700 (lane flow split: 17%, 33%, 50%), and 4050 (lane flow split: 18%, 41%, 41%);

**Four lanes:** Equal lane flows with total flow rates of 450, 900 and 1350 veh/h per lane; unequal flow cases with total flow rates of 1800 veh/h (lane flow split: 17%, 17%, 33%, 33%), and 3600 (lane flow split: 13%, 25%, 25%, 37%), 5400 (lane flow split: 19%, 19%, 31%, 31%);

### Calibration results

The following parameter values were found for the calibrated M3A model.

Single-lane case:

$$\Delta = 1.5 \text{ s} \quad \text{and} \quad b = 0.6 \quad (8a)$$

Multi-lane cases:

$$\Delta = 0.5 \text{ s} \quad \text{and} \quad b = 0.5 \quad \text{for } 2 \text{ lanes} \quad (8b)$$

$$\Delta = 0.5 \text{ s} \quad \text{and} \quad b = 0.8 \quad \text{for } > 2 \text{ lanes} \quad (8c)$$

Headway distributions for equal and unequal lane utilisation in multi-lane cases did not indicate any significant differences. Therefore, the simple method of treating all lanes as a single traffic stream (using the total flow in equations) appears to be a satisfactory method for the prediction of arrival headways for multi-lane cases.

The parameters for Models M1, M2 and M3A given in *Equations (4), (5), and (8a) to (8c)* are summarised in *Table 1*. The proportions of free (unbunched) vehicles predicted using *Equations (6) to (8c)* for single-lane and multi-lane flows are shown in *Figures 1a to 1c* together with the corresponding observed (field and simulation) data. Predicted vs measured cumulative arrival headway probabilities,  $F(t)$ , for the single-lane case are shown in *Figure 1d*.

**Table 1**

#### Summary of parameter values for various headway distribution models

Number of lanes in traffic stream	Negative exponential model (M1)		Shifted negative exponential model (M2)		Bunched exponential model (M3A)		
	$\Delta$	$\varphi$	$\Delta$	$\varphi$	$\Delta$	$\beta$	$\varphi$
1	0	1.0	1.5	1.0	1.5	0.6	$e^{-0.9 q}$
2	0	1.0	0.5	1.0	0.5	0.5	$e^{-0.25 q}$
> 2	0	1.0	0.5	1.0	0.5	0.8	$e^{-0.4 q}$

- For the M3T model, use  $\varphi = 1 - \Delta q$  with same  $\Delta$  values as model M3A.
- Normally, the shifted negative exponential model (M2) is used for single-lane traffic only.

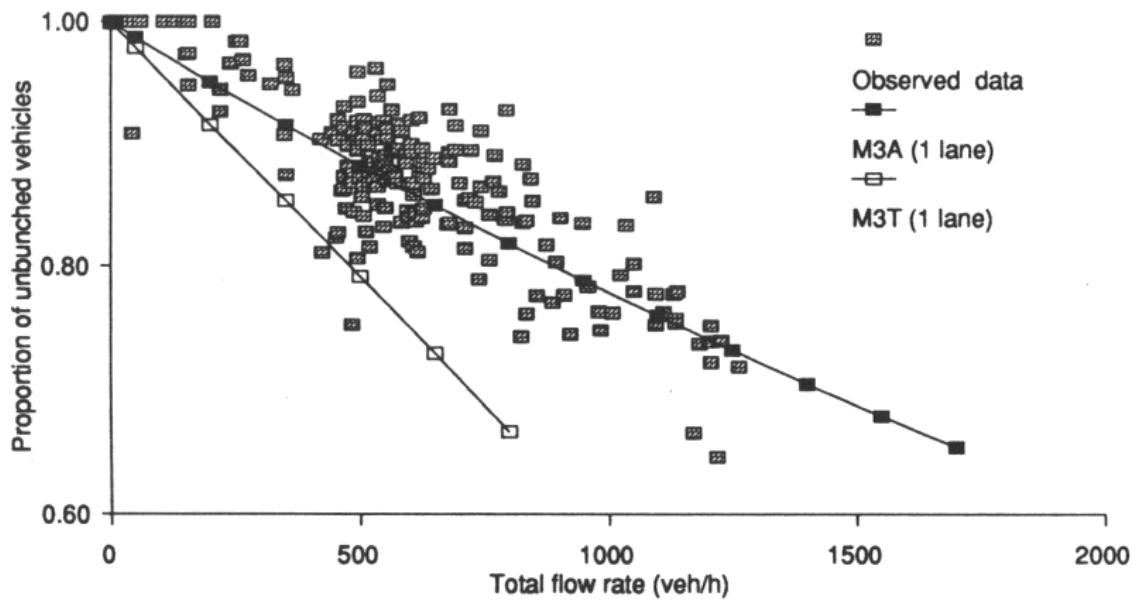


*Figure 1a - Proportion of unbunched (free) vehicles ( $\phi$ ) for 1-lane uninterrupted traffic streams as a function of the total flow ( $q$ ): field data and predictions for M3A and M3T models*

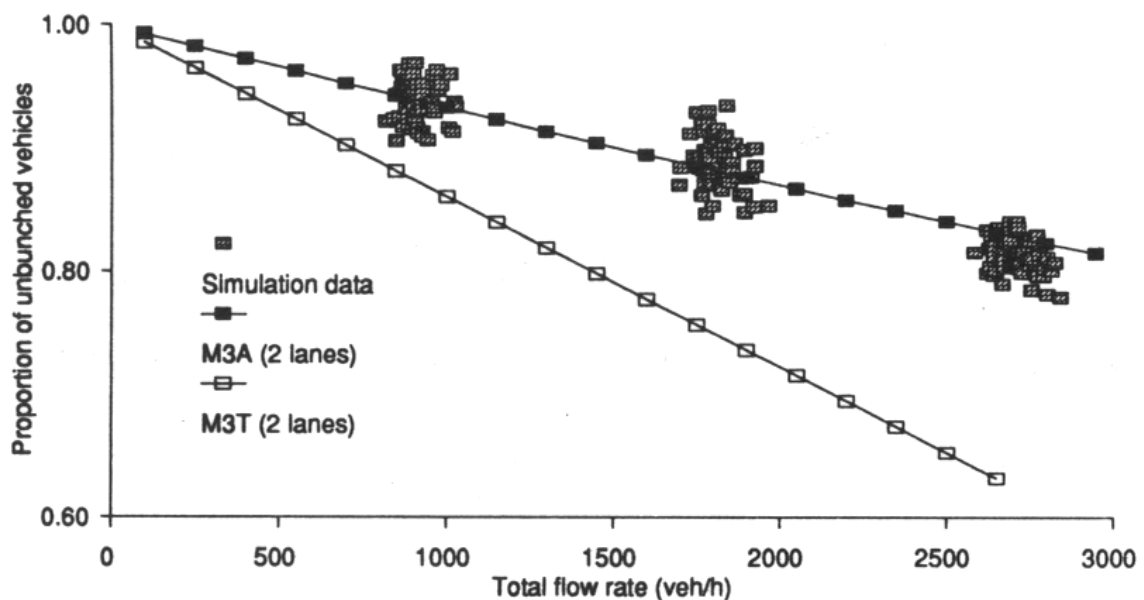


*Figure 1b - Proportion of unbunched (free) vehicles ( $\phi$ ) for 2-lane uninterrupted traffic streams as a function of the total flow in all lanes ( $q$ ): simulation data and predictions for M3A and M3T models*

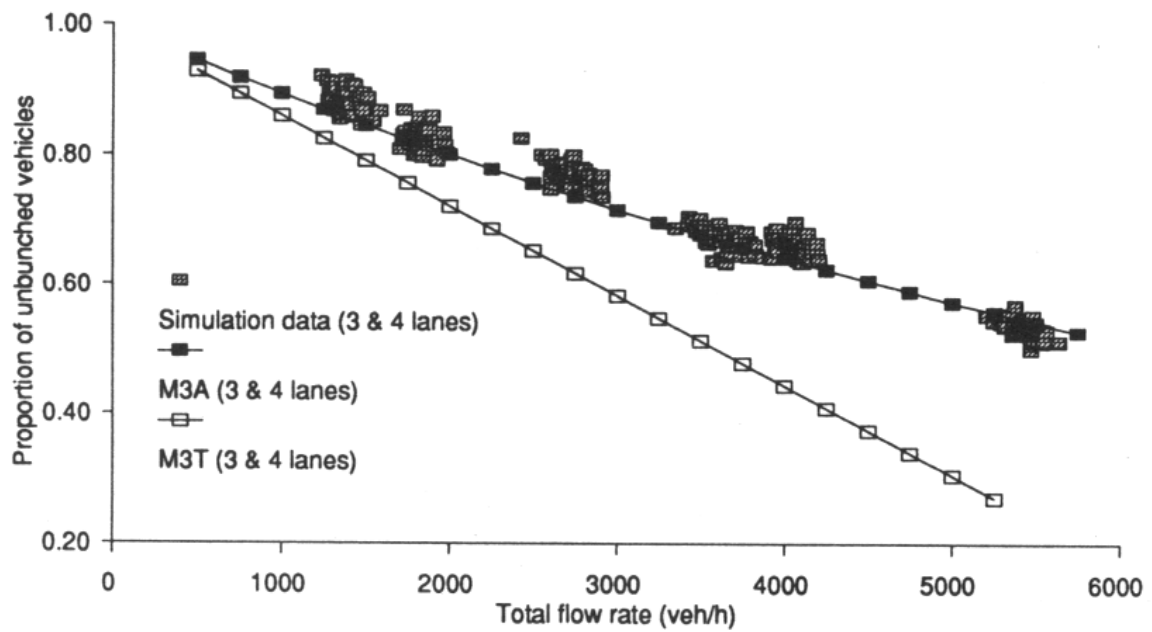


**Figure 1c - Proportion of unbunched (free) vehicles ( $\phi$ ) for 3-lane and 4-lane uninterrupted traffic streams as a function of the total flow in all lanes ( $q$ ): simulation data and predictions for M3A and M3T models**

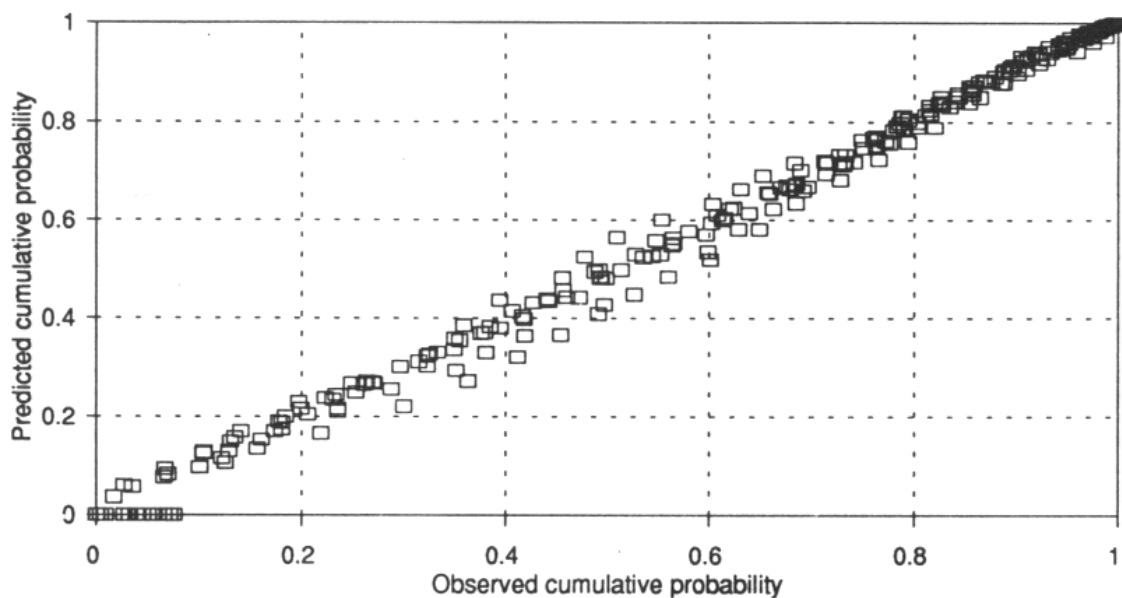


**Figure 1d - Predicted vs measured cumulative arrival headway probabilities,  $F(t)$ , for single-lane traffic streams**

## Discussion

It is seen that *Equations (8a) to (8c)* indicate lower levels of bunching than those predicted by Tanner's linear model (*Equation 7*) and those used previously (Akçelik 1994). It is also seen that it would be possible to use more general linear models to represent real-life data more effectively than Tanner's linear model.

The calibrated model predicts rather high values of  $\phi$  at high flows. The real-life data for the single-lane case did not include very high arrival flow rates since it was difficult to find sites that operate under such conditions (maximum average 15-min flow rate observed was 1264 veh/h). Since, by definition, all vehicles are expected to be bunched when the arrival flow rate equals  $1 / \Delta$ , some improvement to the model for near-capacity conditions should be considered in future research. A two-regime model, a sudden change in the nature of the relationship near capacity (similar to speed-flow models) and even a change in the value of  $\Delta$  as the flows approach uninterrupted flow capacity are the possibilities to explore for this purpose. In this context, it should be noted that  $1 / \Delta$  using the minimum headway value ( $\Delta$ ) determined for the uncongested flow conditions does not necessarily represent the uninterrupted flow capacity.

Flow conditions approaching uninterrupted flow capacities correspond to very poor levels of services for most urban traffic analyses, and may not be easy to find in practice due to other constraints on flows. However, research on this topic would be useful in understanding some fundamental properties of traffic flows.

An interesting observation from the field surveys was that the arrival headway distributions at Sites 1 and 2 (midblock free flow sites) and at Site 5 (the stop line of a busy signalised intersection) were virtually identical (with similar speed limits and same average arrival flow rate).

## Roundabout circulating streams

In SIDRA 4.07 and earlier versions, as in the new AUSTRROADS (1993) roundabout guide, all lanes of the circulating flow are treated as a single stream, and the following linear model is used for estimating the proportion of free vehicles in the circulating stream:

$$\phi_c = 0.75 (1 - \Delta q_c) \quad \text{for } q_c < 1 / \Delta \quad (9)$$

where  $q_c$  is the circulating flow rate (veh/sec). Intra-bunch headways of  $\Delta = 2.0$  s for single-lane circulating roads and  $\Delta = 1.0$  s for multi-lane circulating roads are used.

The data used for the derivation of *Equation (9)* is listed in ARRB Special Report SR 45 (Troutbeck 1989). Using this data,  $b = 2.5$  was chosen for both single-lane and multi-lane circulating flows (as in *Equation 9*) since the differences between  $b$  values for single-lane and multi-lane cases were found to be small. Note that, this calibration was based on the use of the same intra-bunch headways as for *Equation (9)* since the headway data were not available for full calibration of the model. Thus, for roundabout circulating streams:

$$\phi_c = e^{-2.5 \Delta q_c} \quad (10)$$

where  $\Delta = 2.0$  s for single-lane and  $\Delta = 1.0$  s for multi-lane cases.

[Note (June 2003): For roundabout circulating streams, more recent versions of aaSIDRA use  $\Delta = 1.2$  s for two lanes and  $\Delta = 1.0$  s for more than two lanes.]

Figures 2a and 2b show the proportions of free (unbunched) vehicles predicted using Equation (10) for single-lane and multi-lane circulating flows at roundabouts together with the corresponding observed (SR 45) data and the estimates from the linear model (Equation 9).

Equations (9) and (10) predict higher levels of bunching compared with those predicted by Equations (8a) to (8c). The difference can be explained by vehicles entering the circulating stream from queues at roundabout approaches.

Note: For predicting delays, queue length and stop rates for roundabout entry streams, arrival headway distributions based on the parameter values given in Equations (8a) or Table 1 (single-lane cases) are used.

### Examples

Figure 3 shows the *observed* cumulative headway probabilities for a single-lane case with an average arrival flow rate of 1150 veh/h (field data from Sites 1 and 2), as well as the corresponding *predictions* by the arrival headway models M1 ( $\Delta = 0$ ), M2 ( $\Delta = 1.5$ s), M3A ( $\Delta = 1.5$  s,  $b = 0.6$ ) and M3T ( $\Delta = 1.5$  s) calculated from Equations (1) to (8).

Similarly, Figure 4 shows observed cumulative headway probabilities (data from simulation) for a four-lane case with a total arrival flow rate of 3600 veh/h, as well as the corresponding predictions by the arrival headway models M1 ( $\Delta = 0$ ), M2 ( $\Delta = 0.5$  s), M3A ( $\Delta = 0.5$  s,  $b = 0.8$ ) and M3T ( $\Delta = 0.5$  s).

Figures 5a and 5b show examples of cumulative distribution and probability density functions for a single-lane case (arrival flow rate = 1200 veh/h) for the arrival headway models M1 ( $\Delta = 0$ ), M2 ( $\Delta = 1.5$  s), and M3A ( $\Delta = 1.5$  s,  $b = 0.6$ ). For the same single lane case, Figures 6a and 6b show examples of cumulative distribution and probability density functions for model M3 with specified  $\phi$  values of 0.4 for high bunching and 0.9 for low bunching and for model M3A ( $\Delta = 1.5$  s,  $b = 0.6$ ). (Note: in the figures, read *Phi* as  $\phi$ ).

### Discussion

It is seen that there are significant differences in the predictions of arrival headways by different models, especially for small headways. Model M3A is seen to provide good estimates of arrival headways. Generally, the shifted negative exponential model (M2) does not appear to be satisfactory. It is also seen that the amount of bunching as represented by parameter  $\phi$  in model M3 has a significant effect on the prediction of arrival headways.

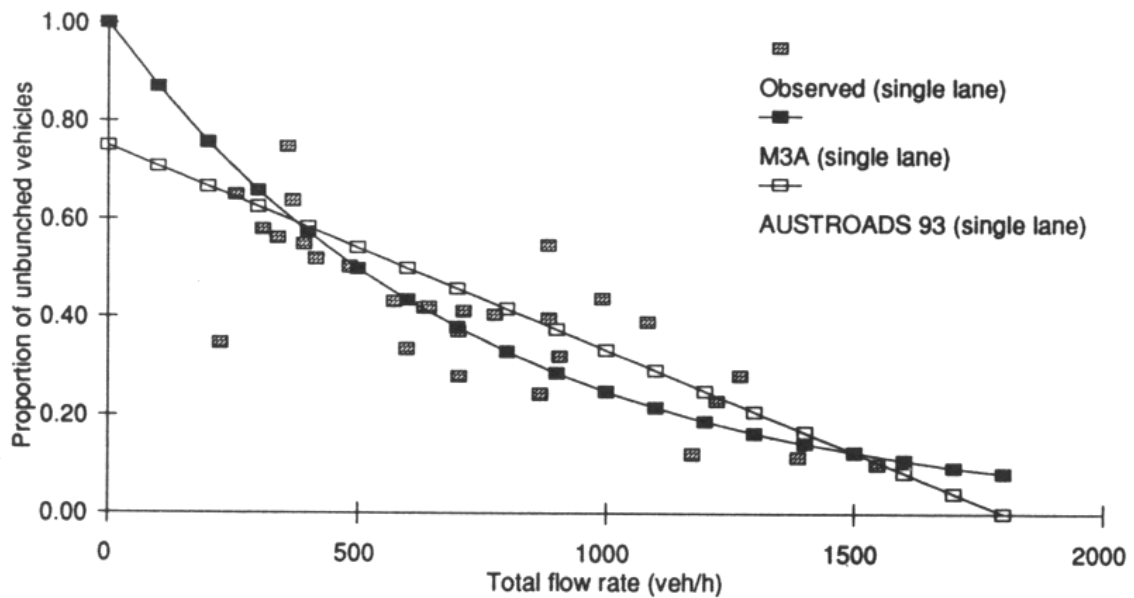


**Figure 2a - Proportion of unbunched (free) vehicles ( $\phi_f$ ) for single-lane circulating streams at roundabouts as a function of the total circulating flow ( $q_c$ ): observed (SR 45) data and predictions for M3A and AUSTROADS (1993) models**

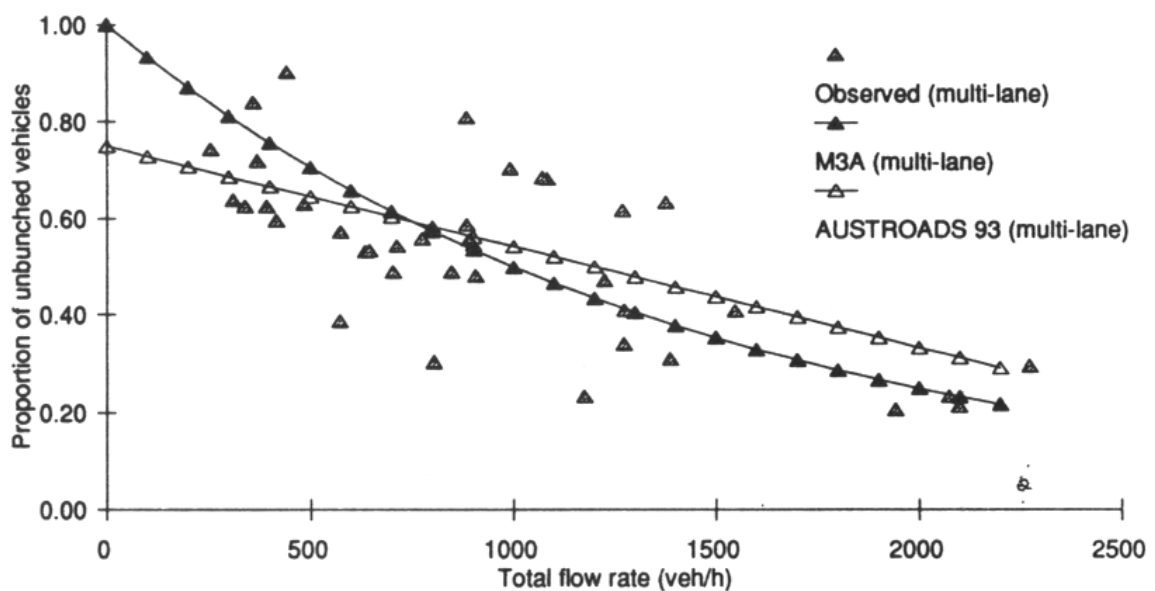


**Figure 2b - Proportion of unbunched (free) vehicles ( $\phi_f$ ) for multi-lane circulating streams at roundabouts as a function of the total circulating flow ( $q_c$ ): observed (SR 45) data and predictions for M3A and AUSTROADS (1993) models**

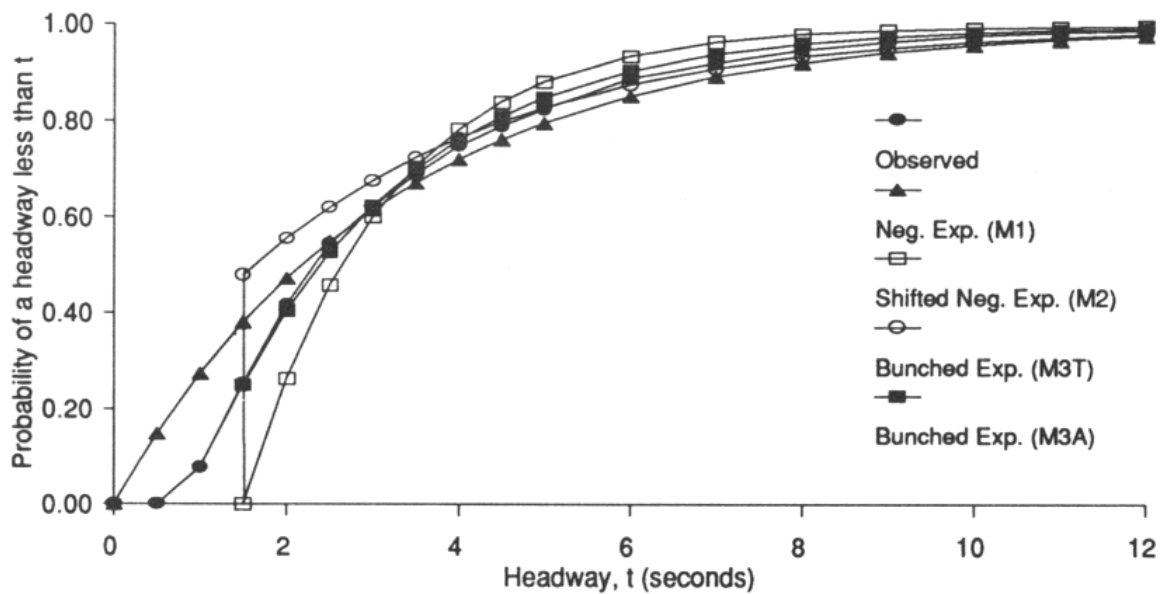


**Figure 3 - Cumulative arrival headway distribution: observed (field) data and predictions by models M1 ( $\Delta = 0$ ), M2 ( $\Delta = 1.5$ ), M3A ( $\Delta = 1.5, b = 0.6$ ) and M3T ( $\Delta = 1.5$ ): single-lane case, average arrival flow rate = 1150 veh/h**

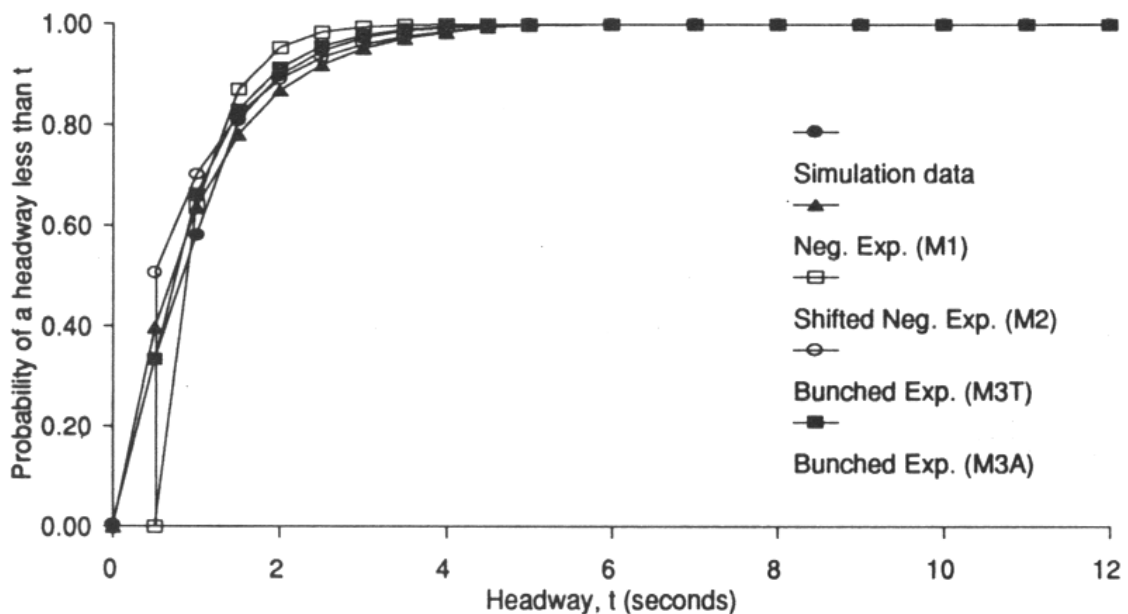


**Figure 4 - Cumulative arrival headway distribution: observed (simulation) data and predictions by models M1 ( $\Delta = 0$ ), M2 ( $\Delta = 0.5$ ), M3A ( $\Delta = 0.5, b = 0.8$ ) and M3T ( $\Delta = 0.5$ ): four-lane case, average arrival flow rate = 3600 veh/h**

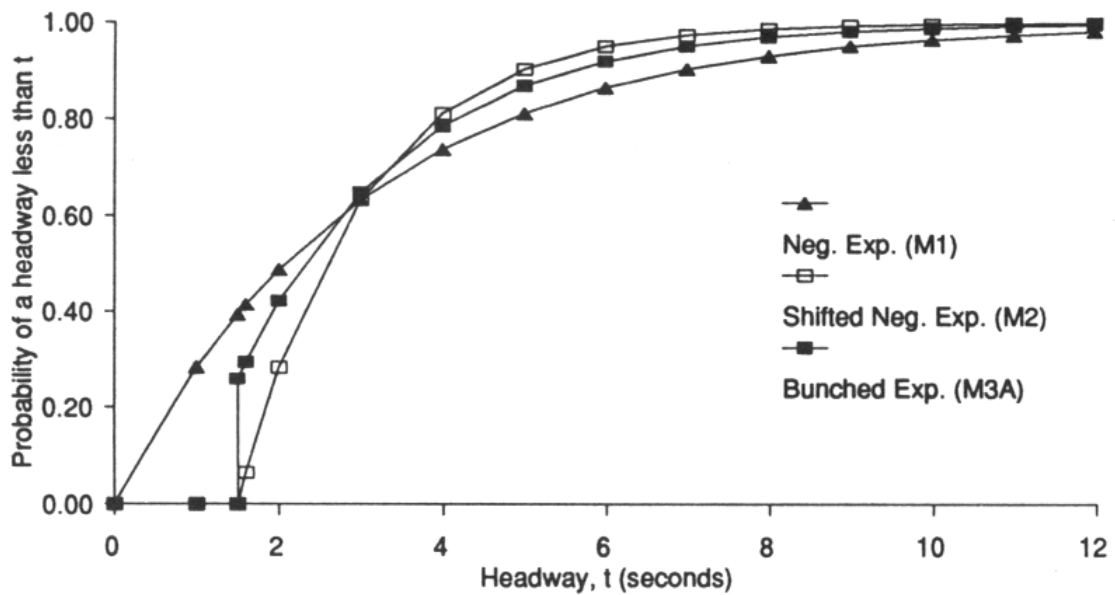


*Figure 5a - Cumulative headway probabilities predicted by models M1 ( $\Delta = 0$ ), M2 ( $\Delta = 1.5$ ), M3A ( $\Delta = 1.5, b = 0.6$ ): single-lane case, arrival flow rate = 1200 veh/h*

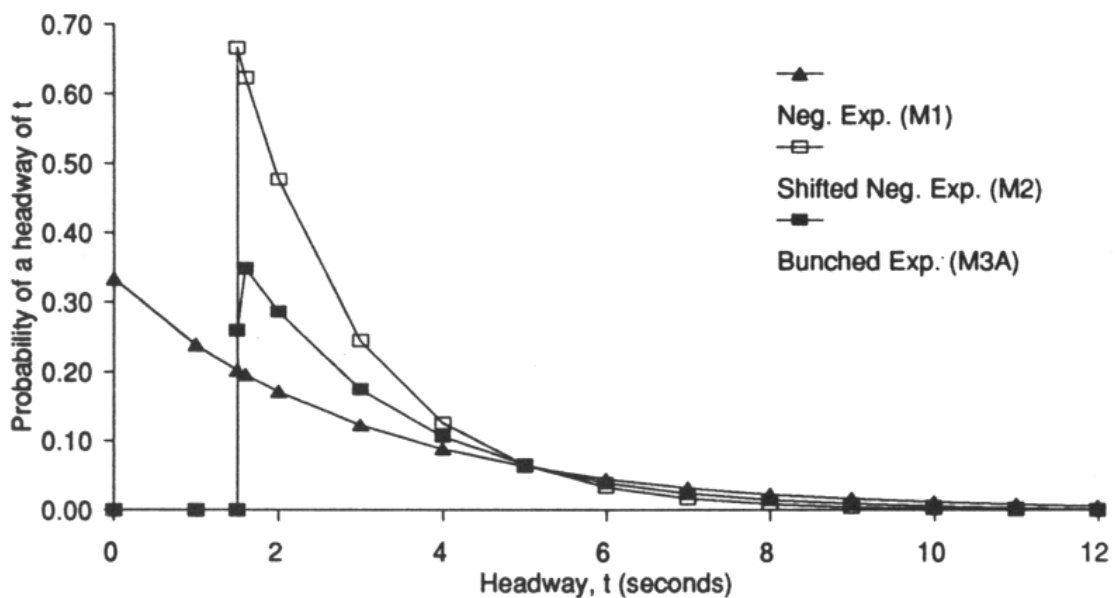


*Figure 5b - Arrival headway probabilities predicted by models M1 ( $\Delta = 0$ ), M2 ( $\Delta = 1.5$ ), M3A ( $\Delta = 1.5, b = 0.6$ ): single-lane case, arrival flow rate = 1200 veh/h (corresponding to cumulative probabilities in Figure 5a)*

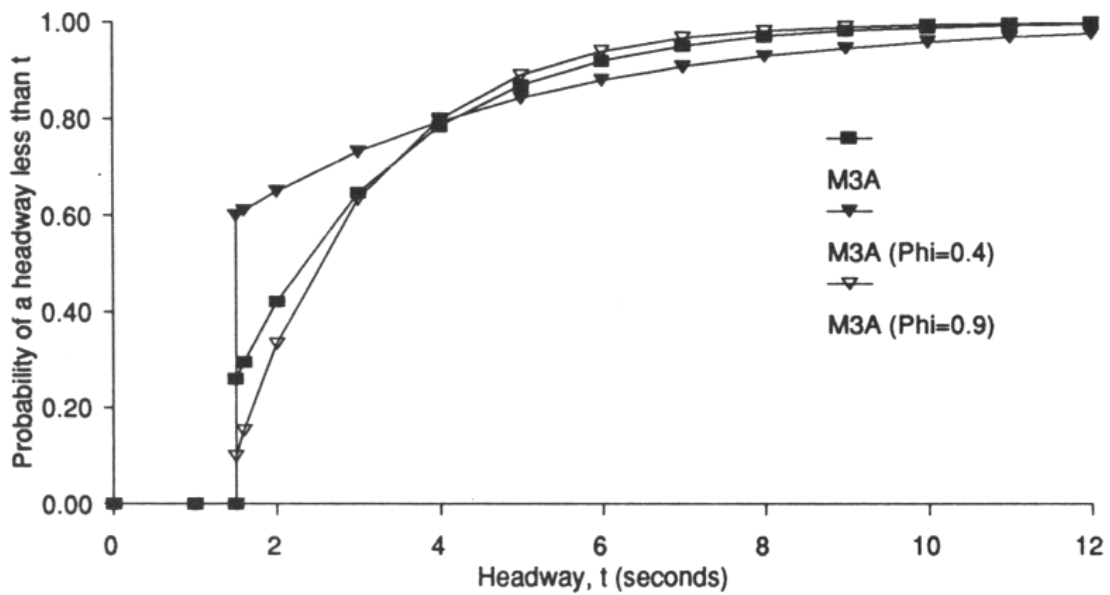


**Figure 6a - Cumulative headway probabilities predicted by model M3 with specified proportions of free vehicles ( $\phi = 0.4$  for high bunching, and  $\phi = 0.9$  for low bunching) and by model M3A ( $\Delta = 1.5$ ,  $b = 0.6$ ): single-lane case with arrival flow rate = 1200 veh/h**

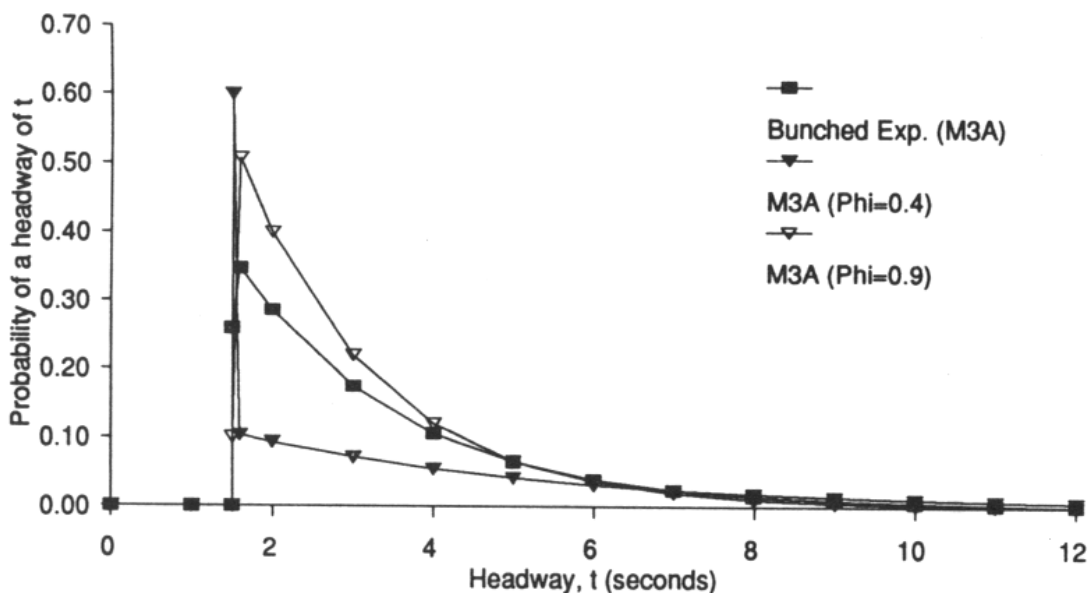


**Figure 6b - Arrival headway probabilities predicted by model M3 with specified proportions of free vehicles ( $\phi = 0.4$  for high bunching, and  $\phi = 0.9$  for low bunching) and by model M3A ( $\Delta = 1.5$ ,  $b = 0.6$ ): single-lane case with arrival flow rate = 1200 veh/h (corresponding to cumulative probabilities in Figure 6a)**

## Gap-acceptance capacities and delays using different exponential headway distributions

Formulae for estimating the average number of arrivals and average headway before a gap change, and the corresponding average green extension time at actuated signals using the bunched exponential headway distribution are given in Akçelik (1994, 1995). Significant differences were found in average green times and cycle times predicted using different arrival headway distributions (models M1, M2, and M3A) and different bunching levels in model M3. In this paper, another area of application, namely the prediction of gap-acceptance capacities and delays will be discussed as an example to indicate the impact of different arrival headway distributions. In this example, capacities and delays for a left-turning vehicle stream (*minor* or *opposed* movement) which gives way to through traffic (*major* or *opposing* movement) at an intersection controlled by a give-way (yield) sign will be considered. All capacity and delay calculations are carried out for individual lanes of minor movements.

### Gap-acceptance capacity

The general capacity model for gap-acceptance processes when each lane of the major (opposing) movement is treated separately (Tanner 1967; Troutbeck 1986, 1989, 1991) was adopted in SIDRA 4.07 in the form of the following formula with the introduction of a minimum capacity concept (Akçelik 1991):

$$Q = \max(Q_g, Q_{\min}) \quad (11)$$

$$Q_g = 3600 \lambda \theta e^{-\lambda(\alpha - \Delta)} / (1 - e^{-\lambda\beta}) \quad \text{for } q_t > 0 \quad (11a)$$

$$= 3600 / \beta_o \quad \text{for } q_t = 0$$

$$Q_{\min} = \min(q_e, 60 n_m) \quad (11b)$$

where

$Q$  = entry capacity of the minor movement (veh/h),

$Q_g$  = capacity estimate using the gap acceptance technique (veh/h),

$Q_{\min}$  = minimum capacity (veh/h)

$n_m$  = minimum number of vehicles per minute which can enter the major traffic stream under heavy opposing flow conditions

$q_e$  = minor movement flow (veh/h)

$q_t$  = total arrival flow in all lanes of the major movement (veh/s)

$\alpha, \beta$  = mean critical gap and follow-up headway for the minor movement (entry stream)(seconds),

$\beta_o$  = follow-up headway when the major movement flow rate is zero ( $\beta = \beta$  for constant follow-up headways)

$\Delta$  = intra-bunch (minimum) headway in a major movement *lane* (seconds); and

$\lambda, \theta$  = parameters for the major movement calculated from:

$$\lambda = \sum \lambda_i \quad (11c)$$

$$\lambda_i = \phi_i q_i / (1 - \Delta q_i) \quad (11d)$$

$$\theta = \Pi (1 - \Delta q_i) \quad (11e)$$

*subject to  $q_i \leq 0.98 / \Delta$  (if  $q_i > 0.98 / \Delta$ , set  $q_i = 0.98 / \Delta$ )*

The summation and multiplication are for the major movement lanes  $i = 1$  to  $n$  ( $n =$  number of major movement lanes),  $\varphi_i =$  proportion of free (unbunched) vehicles in  $i$ th major movement lane, and  $q_i =$  flow rate in  $i$ th major movement lane (*veh/s*); the total opposing flow,  $q_t = \sum q_i$ . The upper limit of  $q_i = 0.98 / \Delta$  was introduced in SIDRA to enable the calculation of non-zero values of  $\lambda$  and  $\theta$  when the major movement flow rate approaches  $1 / \Delta$ .

The general capacity model expressed by Equation (11) is also applicable to the case of *several opposing movements*. In this case, Equations (11c) to (11e) are applied for each lane of all opposing movements consecutively.

The gap-acceptance capacity can be expressed as follows when traffic in all lanes of the major movement is treated together as one stream, i.e. not lane by lane, as in the case of current AUSTRROADS and SIDRA 4.07 models for roundabouts:

$$\begin{aligned} Q_g &= 3600 \varphi q_t e^{-\lambda(\alpha - \Delta)} / (1 - e^{-\lambda\beta}) && \text{for } q_t > 0 \\ &= 3600 / \beta_0 && \text{for } q_t = 0 \end{aligned} \quad (12)$$

where

$$\lambda = \varphi q_t / (1 - \Delta q_t) \quad (12a)$$

*subject to  $q_t \leq 0.98 / \Delta$  (if  $q_t > 0.98 / \Delta$ , set  $q_t = 0.98 / \Delta$ )*

For a single-lane major movement, Equations (11) and (12) give the same result. For multi-lane cases, the intra-bunch headway ( $\Delta$ ) and proportion of free vehicles ( $\varphi$ ) for use in Equation (11) are for the single lane case (Equation 8a), while  $\Delta$  and  $\varphi$  for use in Equation (12) are for the multi-lane case (Equations 8b and 8c). For model M1, there is no difference between Equations (11) and (12) since  $\Delta = 0$ ,  $\varphi = 1$  and  $\lambda = q_t$ .

The following should be noted about the formulae used in Chapter 8 of the current AUSTRROADS (1988) *Capacity Guide* (Traffic Engineering Practice, Part 2):

- (a) The method used for calculating unsignalised (sign-controlled) intersection capacities is equivalent to the M1 model ( $\Delta = 0$ ,  $\varphi = 1$  and  $\lambda = q_t$ ).
- (b) For roundabouts, the same method as in the NAASRA (1986) *roundabout guide* is described. This method uses the M1 model ( $\Delta = 0$ ,  $\varphi = 1$  and  $\lambda = q_t$ ) for multi-lane circulating streams and the M3T model (Equation 7 for  $\varphi$  with  $\Delta = 2$  s) for single-lane circulating streams.

The new roundabout guide (AUSTRROADS 1993) uses a capacity formula equivalent to Equation (12) using the M3 model with  $\varphi$  predicted using Equation (9).

[Note (June 2003): The gap-acceptance capacity formula used in more recent versions of aaSIDRA differs from Equations (11a) and (12). ]

## Examples

Figure 7a shows entry capacities as a function of the arrival flow rate in the case of a single-lane major movement predicted from Equation (12) using  $\alpha = 4$  s and  $\beta = 2$  s for arrival headway models M1 ( $\Delta = 0$ ), M2 ( $\Delta = 1.5$  s), M3A ( $\Delta = 1.5$  s,  $b = 0.6$ ) and M3T ( $\Delta = 1.5$  s).

Figure 7b shows entry capacities as a function of the arrival flow rate in the case of a two-lane major movement (equal lane flows) predicted from Equation (12) using  $\alpha = 4$  s and  $\beta = 2$  s for arrival headway models M1 ( $\Delta = 0$ ), M2 ( $\Delta = 0.5$  s), M3A ( $\Delta = 0.5$  s,  $b = 0.5$ ) and M3T ( $\Delta = 0.5$  s).

Figure 8 presents a comparison of the minor movement capacities for the case of a two-lane major movement (equal lane flows) predicted using the M3A model with  $\alpha = 4$  s and  $\beta = 2$  s and treating the major movement (a) lane-by-lane:  $\Delta = 1.5$  s,  $b = 0.6$  for each lane in Equation (11) and (b) as a single stream:  $\Delta = 0.5$  s,  $b = 0.5$  for both lanes together in Equation 12.

## Discussion

It is seen that there are significant differences in capacities predicted using different exponential distributions of arrival headways, especially in the case of single-lane major movements and when the major flow arrival rates are high. Differences between capacities predicted by treating the major movement lane by lane and as a single stream are also significant for high major movement flow rates, but not very large.

## Gap-acceptance delay

The following time-dependent delay formula is used in SIDRA 4.07 for estimating delays to entry streams at roundabouts and minor movements at unsignalised intersections (Akçelik 1991; Akçelik and Troutbeck 1991). The formula is based on the steady-state model given by Troutbeck (1986, 1989, 1991).

$$d = d_m + 900 T [(x - 1) + ((x - 1)^2 + 8 k x / (q T))^{0.5}] \quad (13)$$

$$d_m = e^{-\lambda(\alpha - \Delta)} / (\lambda \theta) - \alpha - 1 / \lambda + (\lambda \Delta^2 - 2 \Delta + 2 \Delta \phi) / (2 \lambda \Delta + 2 \phi) \quad (13a)$$

$$k = d_m Q / 3600 \quad (13b)$$

where  $d_m$  = minimum delay experienced by the minor movement vehicles (in seconds),  $T$  = duration of the flow period in hours,  $x$  = degree of saturation in the specified flow period,  $k$  = a delay parameter,  $Q$  is minor movement capacity in veh/h from Equation (11), and the gap acceptance parameters  $\alpha$ ,  $\Delta$ ,  $\lambda$ ,  $\theta$  are as defined in Equation (11) for the lane-by-lane treatment (with  $\phi = \lambda \theta / q_t$ ) and Equation (12) for the single-stream treatment.

The AUSTROADS (1993) roundabout guide uses Equation (13) for the case when the circulating stream is treated as a single stream and the proportion of free vehicles calculated from Equation (9) (also see Akçelik and Troutbeck 1991).

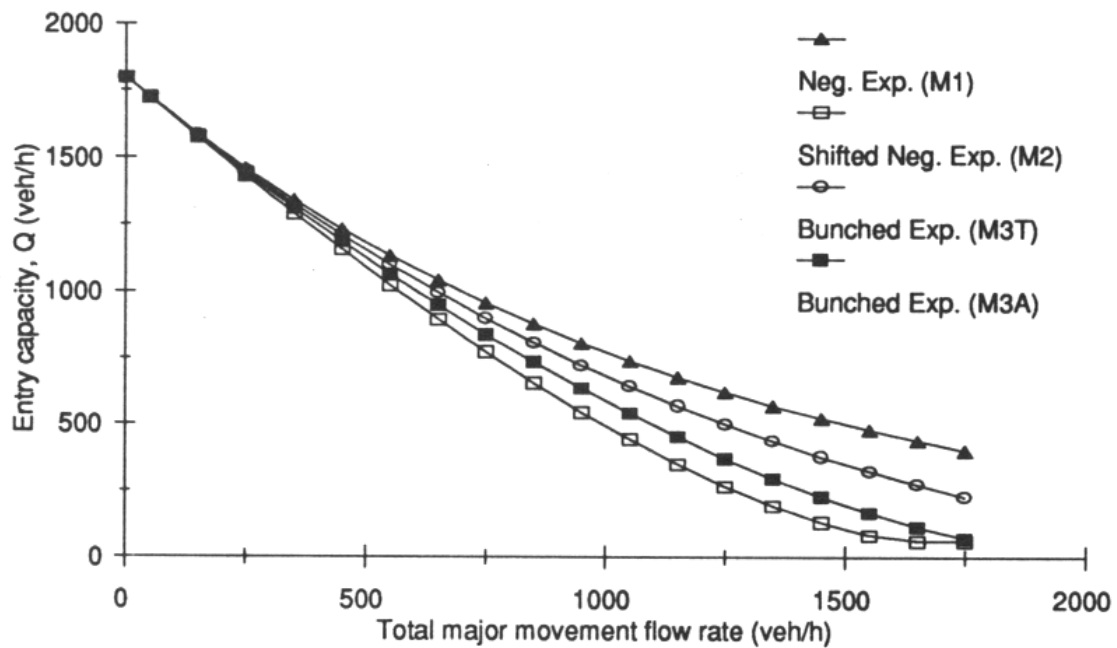


**Figure 7a - Minor movement capacities ( $Q$ ) as a function of the arrival flow of a 1-lane major movement predicted using arrival headway models M1 ( $\Delta = 0$ ), M2 ( $\Delta = 1.5$  s), M3A ( $\Delta = 1.5$  s,  $b = 0.6$ ) and M3T ( $\Delta = 1.5$  s):  $\alpha = 4$  s and  $\beta = 2$  s**

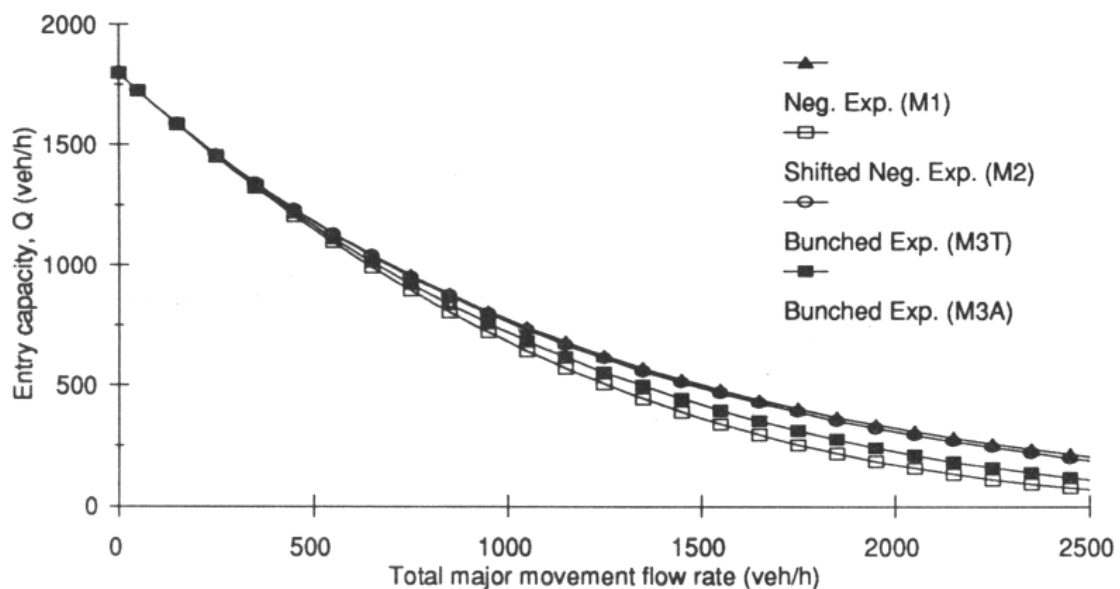


**Figure 7b - Minor movement capacities ( $Q$ ) as a function of the arrival flow of a 2-lane major movement (equal lane flows) predicted using arrival headway models M1 ( $\Delta = 0$ ), M2 ( $\Delta = 0.5$  s), M3A ( $\Delta = 0.5$  s,  $b = 0.5$ ) and M3T ( $\Delta = 0.5$  s):  $\alpha = 4$  s and  $\beta = 2$  s**

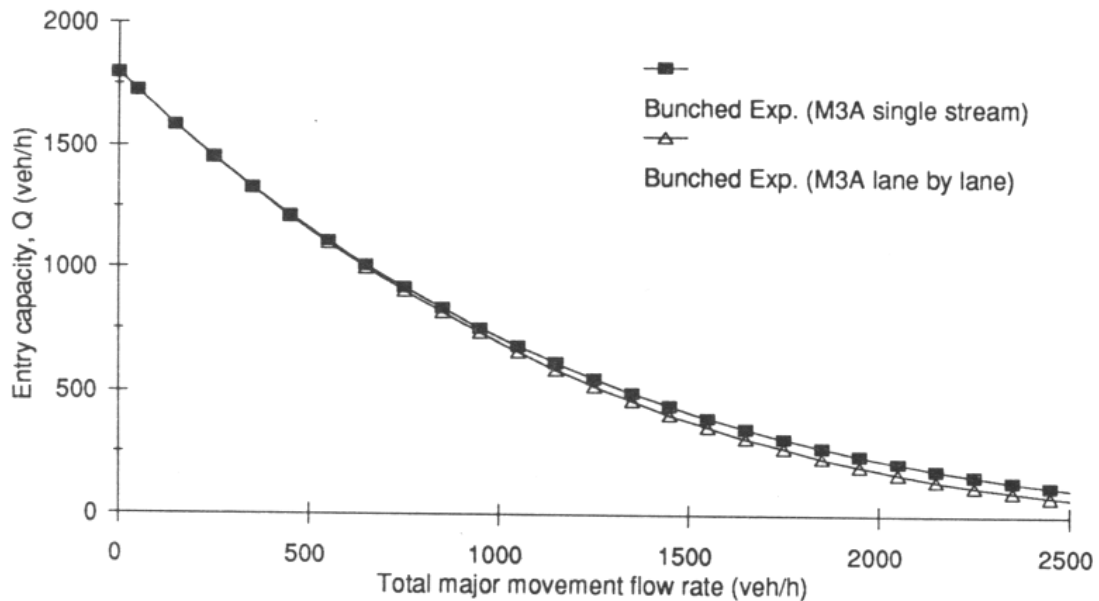


**Figure 8 - Comparison of minor movement capacities ( $Q$ ) for a case of 2-lane major movement (equal lane flows) predicted using model M3A by treating the major movement lane by lane ( $\Delta = 1.5$  s,  $b = 0.6$  for each lane) and as a single stream ( $\Delta = 0.5$  s,  $b = 0.5$ ):  $\alpha = 4$  s and  $\beta = 2$  s**

## Examples

*Figure 9a* shows delays as a function of the minor movement degree of saturation in the case of a single-lane major movement with an arrival flow rate of 900 veh/h predicted using  $\alpha = 4$  s and  $\beta = 2$  s for the arrival headway models M1 ( $\Delta = 0$ ), M2 ( $\Delta = 1.5$  s), M3A ( $\Delta = 1.5$  s,  $b = 0.6$ ) and M3T ( $\Delta = 1.5$  s) for the major movement.

*Figure 9b* shows delays as a function of the minor movement degree of saturation in the case of a two-lane major movement with an arrival flow rate of 900 veh/h per lane, predicted using  $\alpha = 4$  s and  $\beta = 2$  s for the arrival headway models M1 ( $\Delta = 0$ ), M2 ( $\Delta = 0.5$  s), M3A ( $\Delta = 0.5$  s,  $b = 0.5$ ) and M3T ( $\Delta = 0.5$  s) for the major movement.

*Figure 10* presents a comparison of the minor movement delays for the case of a two-lane major movement predicted using the M3A model (same conditions as in *Figure 9b*) and treating the major movement (a) lane-by-lane ( $\Delta = 1.5$  s,  $b = 0.6$  for each lane) and (b) as a single stream ( $\Delta = 0.5$  s,  $b = 0.5$  for both lanes together).

A flow period of  $T = 0.5$  h was used in delay calculations for *Figures 9a*, *9b* and *10*.

As in the case of capacity prediction, it is seen that there are significant differences in delays predicted using different exponential distributions of arrival headways. Differences between delays predicted by treating the major movement lane-by-lane and as a single-stream are small at low flows (as discussed by Troutbeck 1991) but increase with increased flows.

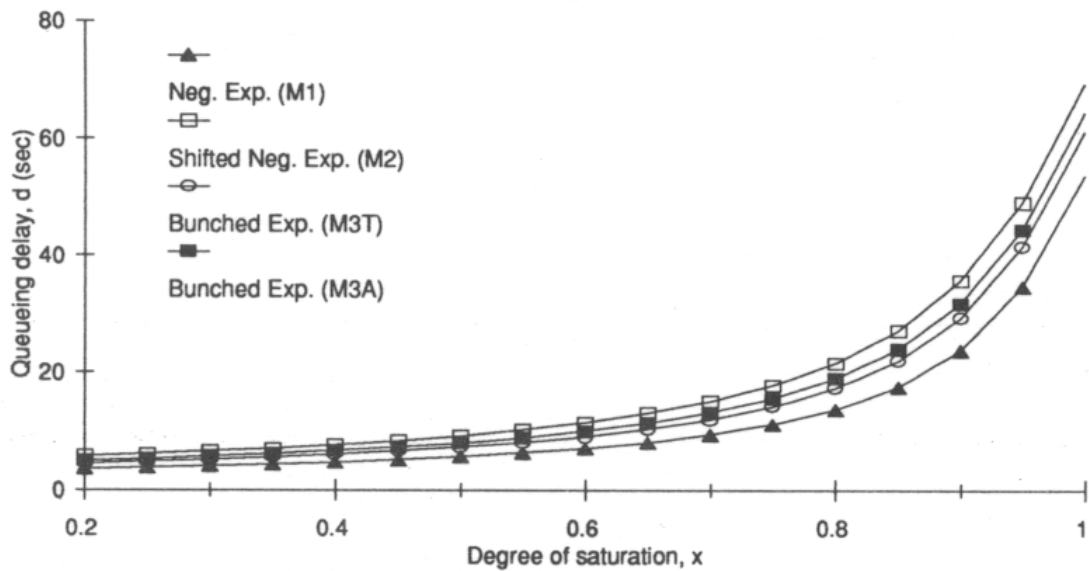


**Figure 9a - Minor movement delays ( $d$ ) as a function of the minor movement degree of saturation ( $x$ ) in the case of a 1-lane major movement (arrival flow rate = 900 veh/h) predicted using the arrival headway models M1 ( $\Delta = 0$ ), M2 ( $\Delta = 1.5$  s), M3A ( $\Delta = 1.5$  s,  $b = 0.6$ ) and M3T ( $\Delta = 1.5$  s):  $\alpha = 4$  s and  $\beta = 2$  s,  $T = 0.5$  h**

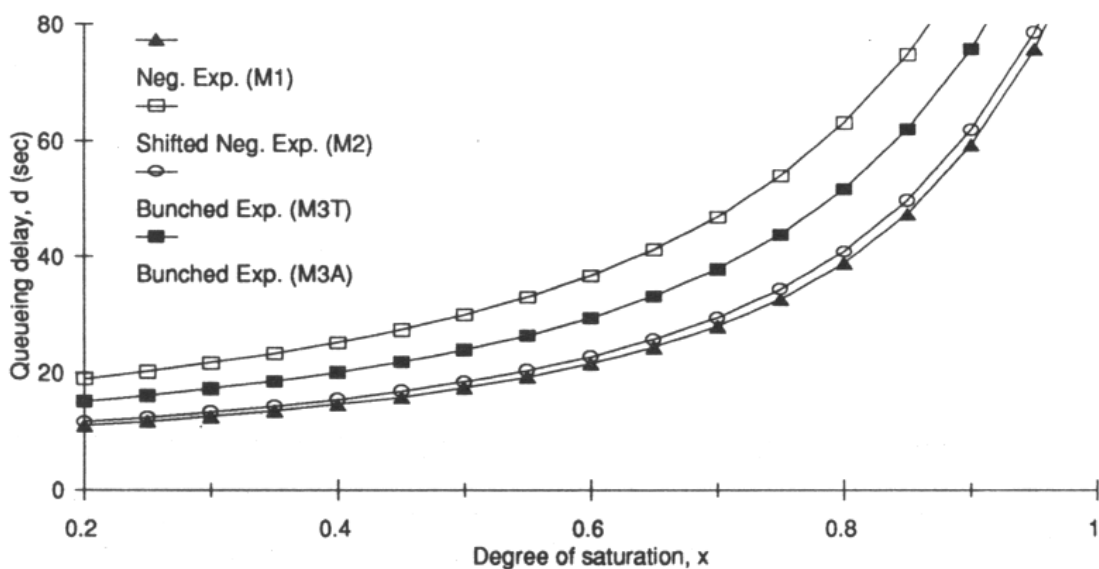


**Figure 9b - Minor movement delays ( $d$ ) as a function of the minor movement degree of saturation ( $x$ ) in the case of a 2-lane major movement (arrival flow rate = 900 veh/h per lane) predicted using the arrival headway models M1 ( $\Delta = 0$ ), M2 ( $\Delta = 0.5$  s), M3A ( $\Delta = 0.5$  s,  $b = 0.5$ ) and M3T ( $\Delta = 0.5$  s):  $\alpha = 4$  s and  $\beta = 2$  s,  $T = 0.5$  h**

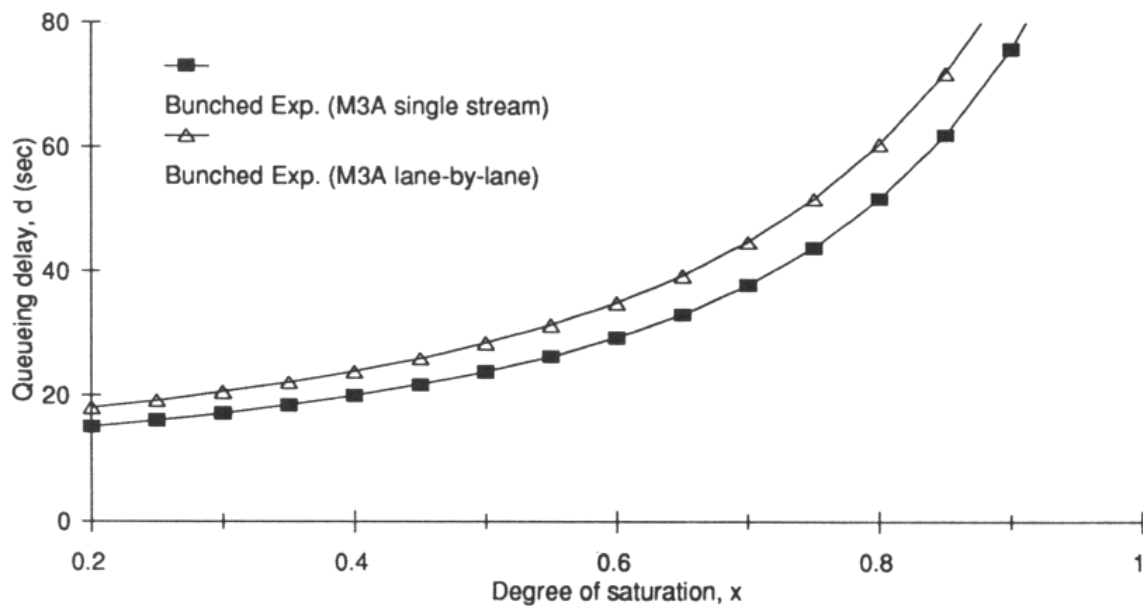


**Figure 10 - Comparison of minor movement delays ( $d$ ) for a case of 2-lane major movement (arrival flow rate = 900 veh/h per lane) predicted using model M3A by treating the major movement lane-by-lane ( $\Delta = 1.5$  s,  $b = 0.6$  for each lane) and as a single stream ( $\Delta = 0.5$  s,  $b = 0.5$ ):  $\alpha = 4$  s and  $\beta = 2$  s,  $T = 0.5$  h**

## Conclusions

The calibration of the model for predicting the proportion of free (unbunched) vehicles indicates lower levels of bunching than those predicted by Tanner's linear model. The new model also predicts rather low values of bunching at high flows compared to Tanner's model. The real-life data did not include very high arrival flow rates as it is difficult to find sites that operate under such conditions. Some improvement to the model for high flow conditions should be considered in future research. A two-regime model, a sudden change in the nature of the relationship near capacity (similar to speed-flow models) and even a change in the value of  $\Delta$  (for better fit) as the flows approach capacity are possibilities to explore for this purpose.

Significant differences were found in capacities and delays predicted using different exponential distributions of arrival headways. Differences between capacities and delays predicted by treating the major movement lane by lane and as a single stream are also significant, but not large.

These findings are in line with other work on actuated signals which indicated that there are significant differences in average actuated signal green times and cycle time predicted using different exponential distributions of arrival headways.

While the bunched exponential distribution of arrival headways is relatively new and its use less common, it has been found to be more realistic. Its use instead of the other two exponential models is strongly recommended. In particular, the more commonly used shifted negative exponential (M2) model is found to give poor predictions for the range of small headways which is of particular interest in the modelling of intersection operations.

## REFERENCES

- AKÇELİK, R. (1981). *Traffic Signals: Capacity and Timing Analysis*. Research Report ARR No. 123. ARRB Transport Research Ltd, Vermont South, Australia. (6th reprint: 1995).
- AKÇELİK, R. (1990). *Calibrating SIDRA*. Research Report ARR No. 180. ARRB Transport Research Ltd, Vermont South, Australia. (2nd edition, 1st reprint 1993).
- AKÇELİK, R. (1991). *Implementing roundabout and other unsignalised intersection analysis methods in SIDRA*. Working Paper WD TE91/002. ARRB Transport Research Ltd, Vermont South, Australia. (Superseded by: AKÇELİK, R., CHUNG, E. and BESLEY, M. (1998). *Roundabouts: Capacity and Performance Analysis*. Research Report ARR No. 321. ARRB Transport Research Ltd, Vermont South, Australia (2nd Edition 1999).)
- AKÇELİK, R. (1994). Estimation of green times and cycle time for vehicle-actuated signals. *Transportation Research Record* 1457, pp 63-72.
- AKÇELİK, R. (1995). *Signal Timing Analysis for Vehicle-Actuated Control*. Working Paper WD TE 95/007. ARRB Transport Research Ltd, Vermont South, Australia.
- AKÇELİK, R. and BESLEY, M. (1992). *SIDRA User Guide*. Working Paper WD TE 91/012. ARRB Transport Research Ltd, Vermont South, Australia. (Superseded by: AKÇELİK & ASSOCIATES (2002). *aaSIDRA User Guide (for version 2)*. Akcelik and Associates Pty Ltd, Melbourne, Australia.)
- AKÇELİK, R. and CHUNG, E. (1994). Traffic performance models for unsignalised intersections and fixed-time signals. In: *Proceedings of the Second International Symposium on Highway Capacity*, Sydney, 1994 (Edited by R. Akçelik). Australian Road Research Board, Volume 1, pp 21-50.
- AKÇELİK, R. and TROUTBECK, R. (1991). Implementation of the Australian roundabout analysis method in SIDRA. In: *Highway Capacity and Level of Service - Proc. of the International Symposium on Highway Capacity*, Karlsruhe, July 1991 (Edited by U. Brannolte). A.A. Balkema, Rotterdam, pp 17-34.
- ASHTON, W.D. (1966). *The Theory of Road Traffic Flow*. Methuen, London.
- AUSTROADS (1988). *Roadway Capacity*. Guide to Traffic Engineering Practice, Part 2. National Association of Australian Road and Traffic Authorities, Sydney.
- AUSTROADS (1993). *Roundabouts*. Guide to Traffic Engineering Practice, Part 6. Australian Association of Australian Road and Traffic Authorities, Sydney.
- BRILON, W. (1988). Recent developments in calculation methods for unsignalised intersections in West Germany. In: *Intersections Without Traffic Signals* (Edited by W. Brilon), Proceedings of an International Workshop, Bochum, Germany, Springer-Verlag, Berlin, pp 111-153.
- COWAN, R.J. (1975). Useful headway models. *Transportation Research* 9 (6), pp 371-375.
- DREW, D.R. (1968). *Traffic Flow Theory and Control*. McGraw-Hill, New York.
- GERLOUGH, D.L. and HUBER, M.J. (1975). *Traffic Flow Theory*. Special Report 165, Transportation Research Board, National Research Council, Washington, D.C.

- GREENSHILDS, B.D. and WEIDA, F.M. (1978). *Statistics with Applications to Highway Traffic Analyses*. ENO Foundation for Transportation, Westport, Connecticut.
- HAIGHT, F.A. (1963). *Mathematical Theories of Traffic Flow*. Academic Press, New York.
- JACOBS, F. (1979). *Capacity calculations for unsignalised intersections* (in German). Vorlesungsmanuskript, Stuttgart.
- LESCHINSKI, R. and ROPER, R. (1993). *VDAS 2000 and 3000 Vehicle Counter and Classifier*. Operating Manual. ARRB Transport Research Ltd, Vermont South, Australia.
- LIN, F-B. (1982a). Estimation of average phase durations for full-actuated signals. *Transportation Research Record* 881, Transportation Research Board, National Research Council, Washington, D.C., pp 65-72.
- LIN, F-B. (1982b). Predictive models of traffic-actuated cycle splits. *Transportation Research* 16B (5), pp 361-372.
- MAY, A.D. (1990). *Traffic Flow Fundamentals*. Prentice Hall, Englewood Cliffs, New Jersey.
- NAASRA (1986). *Roundabouts - a Design Guide*. National Association of Australian State Road Authorities, Sydney.
- SULLIVAN, D.P. and TROUTBECK, R.J. (1993). *Relationship between the Proportion of Free Vehicles and Flow Rate on Arterial Roads*. Physical Infrastructure Centre Report 92-21, Queensland University of Technology, Brisbane.
- TANNER, J.C. (1962). A theoretical analysis of delays at an uncontrolled intersection. *Biometrika*, 49 (1 and 2), pp 163-170.
- TANNER, J.C. (1967). The capacity of an uncontrolled intersection. *Biometrika*, 54 (3 and 4), pp 657-658.
- TROUTBECK, R.J. (1986). Average delay at an unsignalised intersection with two major streams each having a dichotomised headway distribution. *Transportation Science* 20 (4), pp 272-286.
- TROUTBECK, R.J. (1989). *Evaluating the Performance of a Roundabout*. Special Report SR 45. ARRB Transport Research Ltd, Vermont South, Australia.
- TROUTBECK, R.J. (1991). Recent Australian unsignalised intersection research and practices. In: *Intersections Without Traffic Signals II* (Edited by W. Brilon), Proceedings of an International Workshop, Bochum, Germany, Springer-Verlag, Berlin, pp 239-257.